ICES Journal of Marine Science

ICES Journal of Marine Science (2021), 78(1), 112–124. doi:10.1093/icesjms/fsaa197

Original Article

Individual growth profiling improves growth modelling in the geoduck clam *Panopea generosa*

José Angel Hidalgo-de-la-Toba [1], Brent Vadopalas[2], Daniel Bernardo Lluch-Cota[1], Enrique Morales-Bojórquez[1], J. Jesús Bautista-Romero[1], and Sergio Scarry González-Peláez[1]*

[1]*Centro de Investigaciones Biológicas del Noroeste (CIBNOR), Instituto Politécnico Nacional 195, Col. Playa Palo de Santa Rita Sur, La Paz, B.C.S. 23096, Mexico*

[2]*Washington Sea Grant, University of Washington, 3716 Brooklyn Avenue NE, Seattle, WA 98105, USA*

**Corresponding author: tel: +52 (612) 123 8484ext.3951; fax: +52 (612) 125 3625; e-mail: scarry04@cibnor.mx.*

Hidalgo-de-la-Toba, J. A., Vadopalas, B., Lluch-Cota, D. B., Morales-Bojórquez, E., Bautista-Romero, J. J., and González-Peláez, S. S. Individual growth profiling improves growth modelling in the geoduck clam *Panopea generosa*. – ICES Journal of Marine Science, 78: 112–124.

Received 15 May 2020; revised 25 September 2020; accepted 28 September 2020; advance access publication 8 December 2020.

Contemporary modelling of growth based on shell-length to terminal age (SLTA) in long-lived clams is subject to inaccuracies as a consequence of low representation of early age classes in population samplings. To increase early age representation and improve growth modelling, we implemented an approach that used individual growth profile (IGP) data recorded in shells of the Pacific geoduck (*Panopea generosa*). We compared IGP against SLTA and a combination of both IGP + SLTA data through a multi-model approach for the southernmost known *P. generosa* population. The most parsimonious model for both IGP and IGP + SLTA data sets was the Schnute model, with L_∞ = 127.9 and 122.5 mm, respectively, with the asymptotic phase attained at ∼15 years. For SLTA data alone, the most parsimonious was the Johnson model, with L_∞ = 161.6 mm reaching the asymptotic phase at >25 years. In terms of performance, the IGP and IGP + SLTA data sets informed individual growth models with stronger relationships ($r^2 > 0.9$) and higher modelling efficiency ($ME > 0.9$) than those fitted to SLTA alone ($r^2 = 0.51$; $ME = 0.51$). The results demonstrate that IGP yields reliable information from relatively few organisms, improves the biological knowledge of the population, and increases the accuracy of parameter estimates for better fishery management.

Keywords: geoduck, growth modelling, individual growth profiles, *Panopea generosa*

Introduction

Individual growth in bivalves is typically characterized via measurements of the shell length (SL) and estimations of age at the moment of capture [i.e. SL-at-terminal age (SLTA)], which, in most cases, has been done through the counting of growth marks periodically deposited in the shell (Thompson *et al.*, 1980; Cerrato, 2000). As such, the analysis derived from this information represents only the terminal length and age structures of the individuals captured during sampling. Due to the selectivity of the fishing gear used, there exists a certain propensity to bias for certain lengths (Shaul and Goodwin, 1982; Kilada *et al.*, 2007a; Kilada, 2010). This bias has been frequently observed in individual growth analyses in populations of geoducks, a group of long-lived species where early age classes are frequently absent in biological samples [e.g. *Panopea abbreviata* (Zaidman and Morsan, 2015), *Panopea zelandica* (Breen *et al.*, 1991), *P*anopea *globosa* (Aragón-Noriega *et al.*, 2015; González-Peláez *et al.*, 2015), *Panopea generosa* (Bureau *et al.*, 2002, 2003; Calderon-Aguilera *et al.*, 2010)]. Thus, results of individual growth models based on SLTA data sets are frequently unclear for the first years of development, precisely when the accelerated growth phase occurs.

The growth studies conducted in *P. generosa* are in accord that during the first 10 years the highest growth rate occurs, and

subsequently the rate decreases drastically until the organism ultimately reaches maximum size. Despite this general observation, estimates of asymptotic length reveal it to be a highly variable parameter among geographically close areas, ranging from 135.2–161.0 mm for British Columbia (Bureau *et al.*, 2002; Campbell and Ming, 2003) to 130–173 mm in Washington (Hoffman *et al.*, 2000). In Mexico, the recent development of the *P. generosa* fishery led to a series of studies that characterized geographical distribution (González-Peláez *et al.*, 2013), reproduction (Calderon-Aguilera *et al.*, 2014), phylogenetic relationships (Leyva-Valencia *et al.*, 2015), and individual growth (Calderon-Aguilera *et al.*, 2010). Recent study by Hidalgo-de-la-Toba *et al.* (2015) revealed that the southernmost population of *P. generosa* (Punta Canoas, Mexico; González-Peláez *et al*, 2013) exhibits lower average length, weight, age, and individual growth patterns than conspecifics in the centre of their distribution, likely due to range edge effects (Hidalgo-de-la-Toba *et al.*, 2015).

Because growth estimates are used to quantify the biomass of populations and determine the optimal harvest time (King, 2007), errors due to sampling bias can result in over-exploitation or unnecessary economic loss (Hilborn and Walters, 1992; Chen, 2003). Indeed, Thorson and Simpfendorfer (2009) demonstrated that results of individual growth modelling—even through a strong approach such as multi-model inference (MMI)—can be misleading due to a lack of consideration for underlying biases in the data sets, e.g. small sample sizes and gear selectivity.

Some efforts have been made to balance this gap in the age structure, including the inclusion of length-at-age data from previous studies (Kilada *et al.*, 2007b), an additional sampling focused on younger individuals (Hidalgo-de-la-Toba *et al.*, 2015), and the integration of data obtained from juveniles reared under laboratory conditions (Luquin-Covarrubias *et al.*, 2016). However, conducting additional samplings may be expensive and could still produce misrepresentation of individuals of the first age classes in the population due to interannual variability in recruitment (Gerasimova and Maximovich, 2013) as observed in some populations of *P. globosa* (González-Peláez *et al.*, 2015) and *P. generosa* (Orensanz *et al.*, 2004; Zhang and Hand, 2006). Moreover, the integration of juvenile individuals assists only to improve the growth curve close to the origin; the growth during the first years of development is only a projection from the origin to the first SL-at-age data recorded.

As an alternative to the growth modelling and to compensate the absence of younger individuals as a consequence of sampling bias, as in the case of the geoduck *P. generosa*, here we demonstrate the use of the individual growth profiles (IGP). This method comprises the identification and measure of both internal and external growth marks (annuli) in each individual to recover length-at-age data corresponding to the accelerated growth phase of development, as well as the individual's respective terminal age. The purpose is analogous to that of the back-calculation of fish length, used to estimate lengths at ages not found in the sampled population (Francis, 1990; Smart *et al.*, 2013; D'Alberto *et al.*, 2017). However, the method is based on functions of the ratio of annuli measurements in hard structures [e.g. otoliths (Campana, 1990), scales (Ricker, 1992), and spines (Lessa and Duarte-Neto, 2004)] characterization of the relationship between hard structures and fish lengths. Thus, IGP differs from length back-calculation as the growth marks in the shell are a direct record of length increments, obviating the need for any transformation; therefore, IGP represents longitudinal data (Escati-Peñaloza *et al.*, 2010).

Although external growth marks were the first structures to be used to estimate age and size of bivalves (Weymouth, 1923; Weymouth and McMillin, 1930), their use was discontinued in long-lived clams due to the erosion of the shells, the overlap of marks, and the presence of other non-annual marks (Jones *et al.*, 1978; Thompson *et al.*, 1980; Shaul and Goodwin, 1982). In the process of improving age determination in shells, external marks were discarded for analysis, using only the age estimated at the moment of its capture (i.e. length to terminal age). The aim of this study was to model the entire ontogenetic growth of the geoduck clam *P. generosa* by incorporating the IGP as an alternative and additional information source and to compare its performance against the typical information source consisting of the data of length-at-terminal age.

Material and methods

Data collection

Geoduck samples were collected between March 2011 and January 2012 in Punta Canoas (29°25′N, 115°12′W), on the west coast of the Baja California Peninsula, Mexico. Samples were not collected in December due to adverse environmental conditions that precluded dive fishing operations. Samples were taken from commercial landings conducted through hookah diving at a depth of 10–25 m; geoducks were identified by their siphon holes and removed by loosening the substrate using a water jet directed through a hose connected to a pump. Subsequently, the organisms were dissected to remove the soft tissue and both valves were tagged, washed, and allowed to air dry. The right valves from each individual ($N = 243$) were measured from the posterior margin to the anterior in a straight line using a digital calliper (± 0.1 mm) to obtain the terminal SL. These same samples were used in previous studies: characterization of geoduck growth at the edge of their southern range (Hidalgo-de-la-Toba *et al.*, 2015) and validation of annual periodicity of growth marks through sinusoidal and harmonic functions [(Bautista-Romero *et al.* (2015) and Hidalgo-de-la-Toba *et al.* (2018), respectively].

IGP

The IGP method requires the identification and measure of annual growth marks in the shell to rebuild the growth profile over the life history of an individual (Gimenez *et al.*, 2020). To assure accurate representation of the growth variability in the population, subsamples were selected via randomization based on the uniform distribution.

The shells selected for the IGP method were processed as follows. To protect the outer layer of the shell, epoxy resin was applied in a 2–3-cm wide strip, ∼2–3-mm thick, from the plate region of the ligament to the ventral margin, to both on the inside and outside of the left valves. Once the hardening time of the resin had elapsed (24–48 h), the shells were cut transversely from the ligament plate to the ventral margin (Figure 1a) using a low-speed saw (Buehler® Isomet™) with two diamond blades (IsoMet Series 15LC; 0.3-mm thickness and 102-mm diameter) separated by a 2-mm plastic spacer. The cross-sections (Figure 1b) were washed with 70% alcohol to eliminate impurities and allowed to air dry.

A staining procedure was used to enhance the visibility of annuli as follows: the cross-sections were then submerged in

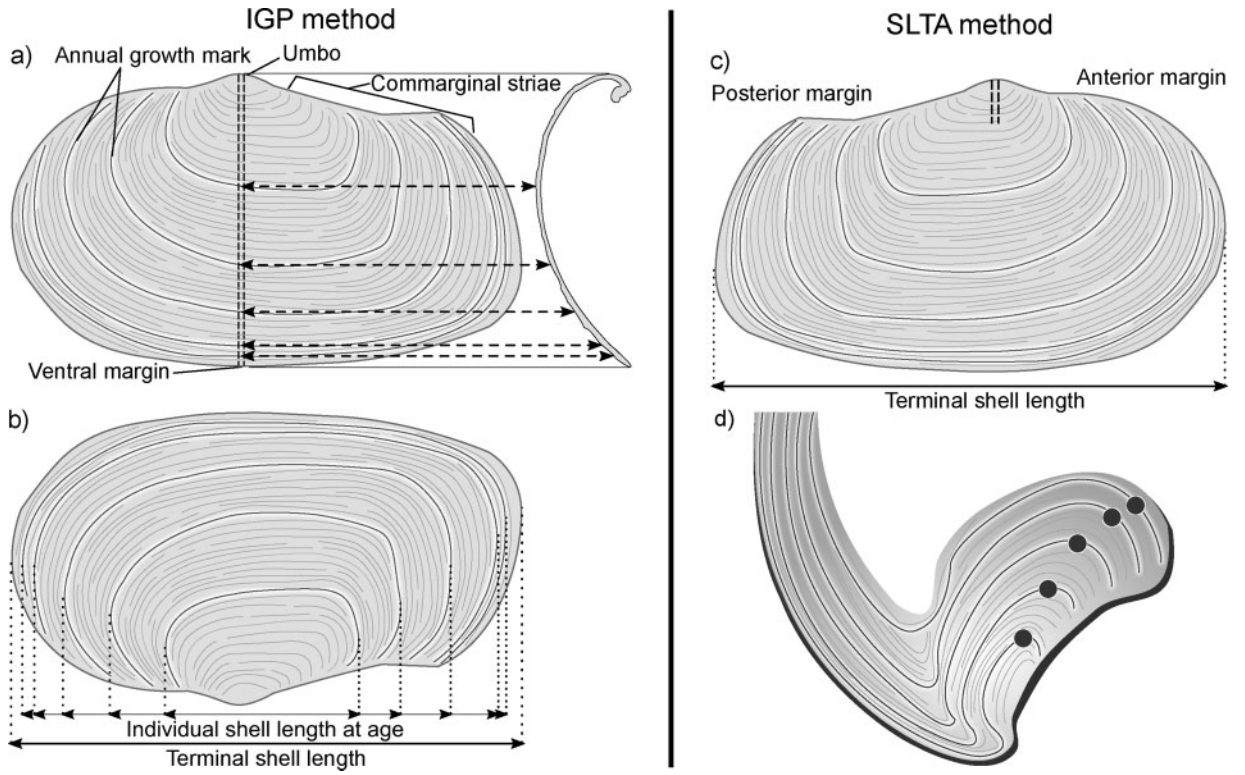

Figure 1. Schematic representation of the procedure of IGP method: (a) left valve of *Panopea generosa* and its respective cross-section; the vertical dashed lines indicate where the cuts were made; the horizontal dashed lines with arrowheads indicate the annual growth marks at different ages identified in the cross-section and their counterpart in the surface of the shell; (b) measurements of both the external annual growth mark on the right valve to determine the individual SL-at-age and its respective terminal SL. Procedure to integrate the SLTA: (c) right valve where the SL was measured from the posterior margin to the anterior in a straight line; the vertical dashed lines indicate where the cuts were made; and (d) cross-section of the ligament plate showing the counting of the internal annual growth marks (•) to determine its final age.

Mutvei's solution [1:1 mixture of 1% acetic acid and 25% glutaraldehyde ($C_5H_8O_2$), with alcian blue ($C_{56}H_{68}Cl_4CuN_{16}S_4$) at saturation (≈7 g/l of solution) (Schöne *et al.*, 2005)] for 30 min at 37°C with constant mixing, then rinsed with distilled water, and allowed to air dry. In this procedure, the acid component slowly removes the carbonate and assists the glutaraldehyde with the stabilization of the organic compound. In the presence of a weak acid, alcian blue functions as a tetravalent cationic dye for acidic sulphated mucopolysaccharides and glycosaminoglycans that had been fixed by the glutaraldehyde.

Using a dissecting microscope at 4×, the lateral view of each cross-section was visualized, individual annuli were identified, and the trajectory of each accelerated growth phase annulus from the ligament plate to where the annulus ended on the outer surface of the left valve was followed (commarginal striae; Figure 2). This process was conducted for all annuli that were quite clear and readily visualized, until succeeding growth increments near the margin were narrow, distorted and/or overcrowded (generally the 10th annulus). The rapid growth during the early growth phase is expressed in wide annuli banding in the shell, in contrast to the extremely narrow banding during later growth. In cases of damaged cross-sections and/or annulus discontinuities, both the sample and data were discarded.

Each annulus was assigned to a chronological age and aligned with the respective external stria in the opposite valve (right valve). Individual SL at age was measured from the posterior margin to the corresponding anterior mark (stria) at the widest point using a digital calliper (±0.1 mm). Thereafter, the IGP of 31 clams were integrated. For each clam the IGP comprised all the identified SL and age data through the period of accelerated growth, as well as the final SL and age attained by the geoduck at the moment of capture, previously defined as SLTA.

SLTA

The traditional source of SL-at-age information used in growth analysis in the species of *Panopea* spp. (Bureau *et al.*, 2002; Campbell and Ming, 2003) was implemented. The terminal age of each individual was observed by counting the internal growth marks in the ligament plate according to Shaul and Goodwin (1982). The umbo region was encased in epoxy and thin-sectioned using the same configuration of the low-speed saw described above. These smaller hinge plate sections were polished with 1200-grit sandpaper and etched with 2% HCl. To enhance the visibility of growth marks, the sections were dusted with a thin layer of graphite powder (González-Peláez *et al.*, 2015). A dissection microscope was used to count the annual growth marks and estimate the terminal age of each clam. The corresponding SL and age data of the full sample ($N = 243$) were integrated in the SLTA data set, including the final SL and age of the subset of clams selected for the IGP method ($n = 31$).

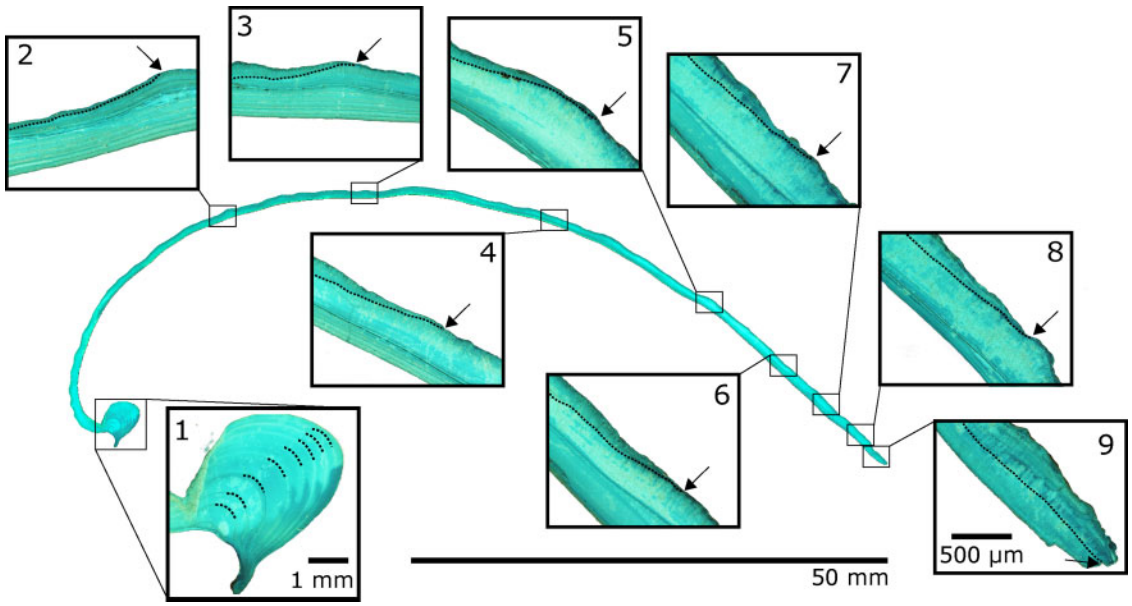

Figure 2. Cross-section of an 8-year-old *Panopea generosa* processed with Mutvei's solution where the ligament plate (1), respective end sites of each annual growth mark in the outer shell surface of the valve (2–8), and annual growth mark of terminal age (9) are shown. Annual growth marks are indicated with dotted lines. The 500-µm scale applies to boxes 2–9.

Reading and accuracy verification

For both aging procedures, IGP and SLTA, two readers examined each sample. In the case of IGP, only complete and readable cross-sections of the left valve were used for the analysis. An inconsistency in the reading of a single growth mark resulted in discarding the sample. On the other hand, in SLTA, the coefficient of variation was estimated according to Chang (1982), for the observations made by the two readers, detailed in González-Peláez *et al.* (2015) and Hidalgo-de-la-Toba *et al.* (2015).

Individual growth modelling

Individual growth was analysed by applying a multi-model inference approach using five candidate asymptotic growth models. The models were fitted separately to each of the data sets previously defined as IGP ($n = 293$) and SLTA ($n = 243$). In addition, growth models were fitted to a third integrated data set comprising both the IGP and SLTA data sets ($n = 505$).

The von Bertalanffy growth model

$$L_t = L_\infty\left(1 - e^{-k(t-t_0)}\right). \tag{1}$$

The Gompertz growth model

$$L_t = L_\infty e\left(-\left({}^{1}/_{k}\right)e^{-k(t-t_1)}\right). \tag{2}$$

The logistic growth model

$$L_t = L_\infty\left(1 + e^{-k(t-t_2)}\right)^{-1}. \tag{3}$$

The Johnson growth model

$$L_t = L_\infty e^{-\left({}^{1}/_{k}*(t-t_0)\right)}. \tag{4}$$

The Schnute growth model (case 1: $\beta \neq 0, \lambda \neq 0$)

$$L_t = \left(y_1{}^{\beta} + \left(y_2{}^{\beta} - y_1{}^{\beta}\right)\frac{1 - e^{-\lambda(t-\tau_1)}}{1 - e^{-\lambda(\tau_2-\tau_1)}}\right)^{{}^{1}/_{\beta}}. \tag{5}$$

For the Schnute growth model, supplementary equations (6 and 7) were used to estimate asymptotic length (L_∞), and theoretical age at length zero (t_0) expressed as follows:

$$L_\infty = \left(\frac{e^{\lambda\tau_2}y_2^{\beta} - e^{\lambda\tau_1}y_1^{\beta}}{e^{\lambda\tau_2} - e^{\lambda\tau_1}}\right)^{{}^{1}/_{\beta}}, \tag{6}$$

$$t_0 = \tau_1 + \tau_2 - \frac{1}{\lambda}\ln\left(\frac{e^{\lambda\tau_2}y_2^{\beta} - e^{\lambda\tau_1}y_1^{\beta}}{y_2^{\beta} - y_1^{\beta}}\right), \tag{7}$$

where k is the growth rate that decreases over time. According to the type of growth model, k decays either linearly (as in von Bertalanffy) or as a non-linear function (as in sigmoidal curves such as Gompertz or Logistic) of size (Ricker, 1979; Katsanevakis, 2006); t_0 is the theoretical age where an individual has a size equal to zero; t_1 and t_2 are points of inflexion; δ is dimensionless factor that confers to the curve a point of inflexion; β is the relative growth constant; λ is the constant of theoretical relative growth; τ_1 and τ_2 are the ages of the youngest and oldest geoducks in the sample, respectively; y_1 and y_2 are the estimated average sizes for those ages.

The growth models were adjusted to the data using the function $-2\ln$ likelihood $\{-2\ln(\ell|\theta i)\}$ (Hidalgo-de-la-Toba *et al.*, 2018).

$$-2\ln(L|\theta i) = n\left[\ln\left(2\pi\frac{\sum_{i=1}^{n}\left(ln\ Lt_o - ln\ Lt_e\right)^2}{n}\right) + 1\right]. \tag{8}$$

The Newton algorithm (Neter *et al.*, 1996) was used to maximize the function $-2\ln(\ell|\theta i)$ and obtain the θ_i parameters for each growth model. In (8), n is the number of observations, and a

multiplicative error was used to stabilize the variance ($\ln Lt_o - \ln Lt_e$).

The confidence intervals (*CI*) were estimated via Monte Carlo simulations. The calculations were based on the method of parametric simulations described by Fournier and Archibald (1982). In addition, the simulations were parametric with residuals sampled from an assumed probability distribution. Subsequently, the simulated data were estimated from a log-normal distribution without bias correction expressed as: $A_s = A_e \times \exp^{\varepsilon_i}$, where A_s is the simulated age, A_e is the estimated age, and $\varepsilon_i \approx N(0, \sigma^2)$ (Pardo *et al.*, 2013). This process creates a new data set with the same statistical properties of the original data, as well as a new set of parameters, which can be used to study the empirical distribution of the estimated parameters. Moreover, the bootstrap standard deviation (SD_B) is an estimate of the standard error (SE) of the θ_t estimate. The bootstrap mean ($-x$) is an estimate of the mean value of the θ_t estimate. Consequently, the coefficient of variation (Ω) was estimated as $\Omega = {}^{sd}/_{-x}$ (Deriso *et al.*, 1985). The bias (B) and percent bias ($\%B$) were estimated as follows: $B = -x - \theta_i$ and $\%B = \frac{-x-\theta_i}{\theta_i} \times 100\%$ (Jacobson *et al.*, 1994), where θ_i is the best *i*th parameter estimate from each candidate growth model fitted to the original data. The upper and lower *CI* were estimated using the bias-corrected percentile method (Haddon, 2011).

Model selection criterion

The Akaike information criterion (*AIC*) and Schwartz-Bayesian criterion (*SBC*) were simultaneously implemented to assist in the selection of the best candidate model and increase model selection certainty: if both criteria are not in accord, it is recommended to continue with the search for candidate models until one that is favoured by both criteria is found (Kuha, 2004).

$$AIC = -2\ln(\ell|\theta i) + 2k, \tag{9}$$

$$SBC = -2\ln(\ell|\theta i) + [\ln(n) \times k], \tag{10}$$

where the k argument is the penalty that the model is given for each θ_i parameter estimated. In addition, *AIC* is an estimator of the relative expected distance between the adjusted model and the observed data. The best candidate model will be the one with the lowest AIC value among all the groups of the candidate models, with the result being favoured over the basis of fit and parsimony (Link and Barker, 2006). *SBC* further penalizes the number of model parameters by applying a term that varies in function of the sample size and the number of parameters, thus selecting a more parsimonious model than *AIC* (Johnson and Omland, 2004; Wang and Liu, 2006; Ward, 2008). The interpretation of the results follows the same logic as *AIC*, where the best candidate model is the one with the lowest *SBC* value.

AIC and *SBC* differences ($\Delta_{i\text{-}AIC}$ and $\Delta_{i\text{-}SBC}$, respectively) were calculated to facilitate the interpretation of both criteria and offer an element of discrimination between the analysed growth models. Here, Δ_i is the difference of value between the *AIC* or *SBC* of each model-*i* (AIC_i; SBC_i) with respect to the *AIC* or *SBC* of the model with the lowest value (SBC_{min}; SBC_{min}) (Burnham and Anderson, 2002).

$$\Delta_{i-AIC} = AIC_i - AIC_{min}, \tag{11}$$

$$\Delta_{i-SBC} = SBC_i - SBC_{min}. \tag{12}$$

Thus, the candidate model that presents a value of $\Delta_i = 0$ corresponds to the best model with the lowest *AIC* or *SBC* value; models with $\Delta_i \leq 2$ offer substantial evidence as an alternative as well as a plausible model for describing the data; the models with Δ_i values ≥ 4 and ≤ 7 have markedly less support; and models with $\Delta_i > 10$ lack evidence supporting their use (Burnham and Anderson, 2002; Barreto *et al.*, 2011).

To obtain the relative plausibility of each model fitted to the data, the percentage of Akaike and Schwartz-Bayesian weights ($w_{i\text{-}AIC}$ and $w_{i\text{-}SBC}$, respectively) were calculated (Burnham, 2004; Katsanevakis, 2006). These are interpreted as the probability that the model selected is indeed the best choice given the data.

$$w_{i-AIC} = \frac{e^{\left(-1/2\Delta_{i-AIC}\right)}}{\sum_{r=1}^{R} e^{\left(-1/2\Delta_r\right)}} \times 100, \tag{13}$$

$$w_{i-SBC} = \frac{e^{\left(-1/2\Delta_{i-SBC}\right)}}{\sum_{r=1}^{R} e^{\left(-1/2\Delta_r\right)}} \times 100. \tag{14}$$

Model assessments

The performance of the most parsimonious model from the three data sets was evaluated through the coefficient of determination (r^2; 15) as a measure of the strength of the model, expressed as the proportion of the data explained by the fitted model. In addition, the modelling efficiency (*ME*; 16) was applied to assess the accuracy of the growth model by comparing its variance with the variance of the mean of the observations. The rationale of the *ME* is that when the predicted values exactly match the measured values, the $ME = 1$. However, if this value is negative, the growth model performs inadequately since it is worse than simply using the observed mean (Loague and Green, 1991; Smith *et al.*, 1996).

$$r^2 = 1 - \frac{RSS}{TSS}, \tag{15}$$

$$ME = \frac{\sum_{i=1}^{n}(L_{obs\ i} - L_{obs})^2 - \sum_{i=1}^{n}(L_{t\ i} - L_{obs\ i})^2}{\sum_{i=1}^{n}(L_{obs\ i} - L_{obs})^2}, \tag{16}$$

where *RSS* is the residual sum of squares; *TSS* is total sum of squares; L_{obs} is the observed SL of the individual *i*; L_t is the SL estimated by the model for the individual *i*, and L_{obs} is the mean of the observed SL.

Analysis of temporal correlation of IGP data

The IGP data correspond to longitudinal data, they are defined as repeated measures data where the observations within individuals were not (or could not have been) randomly assigned to the levels of a "treatment" of interest (age in this study). Therefore, some serial (temporal) correlation among the measurements in an individual specimen is likely. To evaluate this correlation, a nonlinear

mixed effects model was conducted using annual growth increments, $\Delta L_t = L_{t+1} - L_t$, according to Escati-Peñaloza *et al.* (2010). Given that the Schnute growth model was the candidate model selected by *AIC* and *SBC* criteria, then the ΔL_t estimated from IGP data was estimated as follows (Haist, 2018):

$$\Delta L_t = \left[L_t{}^{\beta}\exp^{-\lambda} + L_{\infty}{}^{\beta}(1-\exp^{-\lambda})\right]^{1/\beta} - L_t, \quad (17)$$

where ΔL_t is the expected mean growth increment for SL class at a specific age L_t. The first clearly identifiable annual growth rings were excluded from the analysis because the absolute age associated with them is uncertain due to variability in the time at settlement (Escati-Peñaloza *et al.*, 2010).

The mixed effects model can be expressed as the sum of a population mean parameter (fixed effect) and an individual deviation (random effect) (Lindstrom and Bates, 1990). The growth increments of the *i*th individual were given by:

$$\Delta L_{t,i} = \left[L_{t,i}{}^{(\beta+\beta^{\tau})}\exp^{-(\lambda+\lambda^{\tau})} + (L_{\infty}+l_{\infty i})^{(\beta+\beta^{\tau})}(1-\exp^{-(\lambda+\lambda^{\tau})})\right]^{1/(\beta+\beta^{\tau})} - L_{t,i}, \quad (18)$$

where L_{∞}, β, and λ are parameters of Schnute growth model (fixed effects); l_{∞}, β^{τ}, and λ^{τ} are the parameters including random effects, assumed to be normally distributed, with zero mean and variance–covariance matrix (Ψ_i), expressing a 3×3 matrix according to:

$$\Psi_i = \begin{pmatrix} \sigma^2_{l_{\infty}} & \rho l_{\infty}\beta^{\tau}\sigma_{l_{\infty}}\sigma_{\beta^{\tau}} & \rho l_{\infty}\lambda^{\tau}\sigma_{l_{\infty}}\sigma_{\lambda^{\tau}} \\ \rho l_{\infty}\beta^{\tau}\sigma_{l_{\infty}}\sigma_{\beta^{\tau}} & \sigma^2_{\beta^{\tau}} & \rho\beta\lambda^{\tau}\sigma_{\lambda^{\tau}}\sigma_{\beta^{\tau}} \\ \rho l_{\infty}\lambda^{\tau}\sigma_{l_{\infty}}\sigma_{\lambda^{\tau}} & \rho\beta\lambda^{\tau}\sigma_{\lambda^{\tau}}\sigma_{\beta^{\tau}} & \sigma^2_{\lambda^{\tau}} \end{pmatrix}, \quad (19)$$

where $\sigma^2_{l_{\infty}}$ is the variance of the l_{∞}indicating random effects, $\sigma^2_{\beta^{\tau}}$ represents the variance of β^{τ} exhibting random effects, $\sigma^2_{\lambda^{\tau}}$ indicates the variance of λ^{τ} denoting random effects, the correlations (ρ) between parameters including random effects were estimated by $\rho l_{\infty}\beta^{\tau}$, $\rho l_{\infty}\lambda^{\tau}$, and $\rho\beta\lambda^{\tau}$. The estimates of both models (17 and 18) were fitted to a linear model. The dependence of sequential observations within-individuals was evaluated by estimating the serial autocorrelation of model residuals using a first order auto-regressive function (Escati-Peñaloza *et al.*, 2010); the autocorrelation estimated was analysed by the statistical Box Ljung test function contained in the library "stats" version 1.11-1 from R project software (Ljung and Box, 1978; R Core Team, 2020).The Ljung–Box test ($Q_{\alpha<0.5,\ df=1}$) was assessed following the next hypotheses ($\alpha = 0.05$): null hypothesis indicating that the data are independently distributed and alternative hypothesis indicating that the data are not independently distributed and consequently they exhibit serial correlation.

Results

SL and age structure of the sample

The average SL and age of the whole sample obtained from the commercial catch were 113.8 mm (*SD* = 12.5 mm) and 12.5 years (*SD* = 4.7 years) and ranged from 90.9 to 144.0 mm (Figure 3a) and 4 to 25 years (Figure 3b), which corresponds to the terminal data of the whole sample (SLTA). Furthermore, the sub-sample used to integrate their IGP consisted of 31 geoducks, the average SL was 117.7 mm (*SD* = 12.4 mm) ranged from 95.8 to 140.5 mm (Figure 3a) and the average age was 13.3 years (*SD* = 5.2 years).

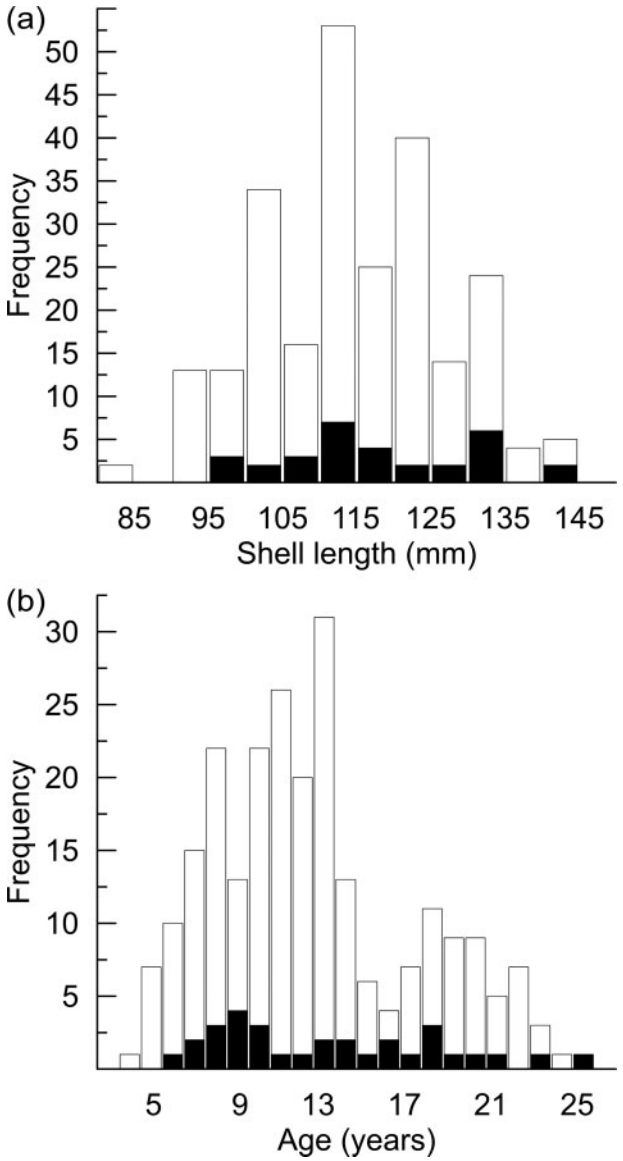

Figure 3. Terminal SL and age frequency distributions of the whole sample of Pacific geoduck *Panopea generosa* from the commercial catch ($n = 243$); black shows the terminal SL and age of the subsample used to estimate the IGP ($n = 31$).

The randomization procedure resulted in a representative subsample that ranged from 6 to 25 years (Figure 3b). The IGP method enabled the visualization and measurement of external marks primarily for ages 1–10 years, with a maximum of ages 1–14 years. Thus, 293 SL-at-age data were generated with the inclusion of the final SL and age attained by the geoduck at the moment of capture (Table 1). The combination of the SL-at-age data from the IGP data set and the 212 SL-at-age data from the SLTA data set (by excluding the 31 individuals which were selected in IGP to avoid data duplication) integrated a total of 505 SL-at-age data (IGP + SLTA data set).

Reading and accuracy verification

As Mutvei's solution is a staining procedure that dramatically enhances the visibility of annuli, inconsistency in the readings of

Table 1. Descriptive statistic of observed SL (mm) by each age class (years) recovered through IGP including the respective SL at terminal age ($n = 293$).

Age	*n*	Mean	SD	Minimum	Maximum
1	25	27.1	4.5	20.3	37.0
2	30	45.7	7.6	28.4	62.2
3	31	62.0	9.4	41.4	77.9
4	31	76.5	11.0	54.3	97.3
5	31	89.4	9.2	70.7	107.4
6	31	98.3	8.4	84.0	116.4
7	30	104.6	8.7	89.6	122.0
8	23	109.5	8.7	93.6	126.7
9	20	112.2	7.6	97.8	125.0
10	14	115.6	7.8	104.6	130.3
11	6	120.8	4.7	115.0	126.7
12	3	122.2	10.2	110.5	128.2
13	3	121.8	11.6	113.0	134.9
14	3	121.7	15.2	110.7	139.1
15	1	120.1	–	120.1	120.1
16	2	122.4	10.9	114.7	130.1
17	1	130.5	–	130.5	130.5
18	3	131.8	3.6	127.7	134.0
19	1	140.4	–	140.4	140.4
20	1	129.7	–	129.7	129.7
21	1	130.2	–	130.2	130.2
22	–	–	–	–	–
23	1	132.9	–	132.9	132.9
24	–	–	–	–	–
25	1	140.5	–	140.5	140.5

n, data number.

IGP only occurred on the first one or two annuli of six of the 31 samples analysed. We were able to determine that erosion of the first annual growth marks in these individuals limited the precise identification of their end points. Thus, the discrepancy between both readers was essentially zero. For SLTA, the *C.V.* of the aging procedure in cross-sections of the ligament plate was 2.62%.

IGP modelling

Each of the models using the IGP data set described a similar pattern of growth in the first years of development of the individuals; however, clear differences among models were observed as growth approached the asymptotic SL (Figure 4a). The logistic model showed the lowest asymptotic SL value among the candidate growth models ($L_\infty = 116.7$ mm); the asymptotic phase was reached at around 10 years of age. In contrast, the Johnson growth model described a greater asymptotic SL ($L_\infty =$ 171.4 mm) for ages older than those found in the population; this model suggested that the asymptotic phase is reached at over 25 years. The Gompertz, Schnute and von Bertalanffy models described asymptotic SLs between 122.5 and 135.0 mm, with the asymptotic phase reached at ages over 15 years (Table 2).

The *AIC* and *SBC* were in accord that the best growth model was Schnute ($w_{i\text{-}AIC} = 94.4\%$; $w_{i\text{-}SBC} = 72.6\%$). There was a lack of concordance, however, between the two criteria regarding the von Bertalanffy and Gompertz models. The *AIC* indicated that the von Bertalanffy and Gompertz models were relatively poorly supported by the data ($\Delta_i = 6.9$ and 7.2, respectively), whereas the SBC results ($\Delta_i = 3.2$ and $\Delta_i = 3.5$, respectively) indicated that these two models were plausible descriptors of the individual growth in this population. The *AIC* and *SBC* were concordant in their lack of support for both the Johnson and Logistic models (AIC $\Delta_i = 17.6$ and 51.3; SBC $\Delta_i = 13.9$ and 17.6, respectively; Table 3).

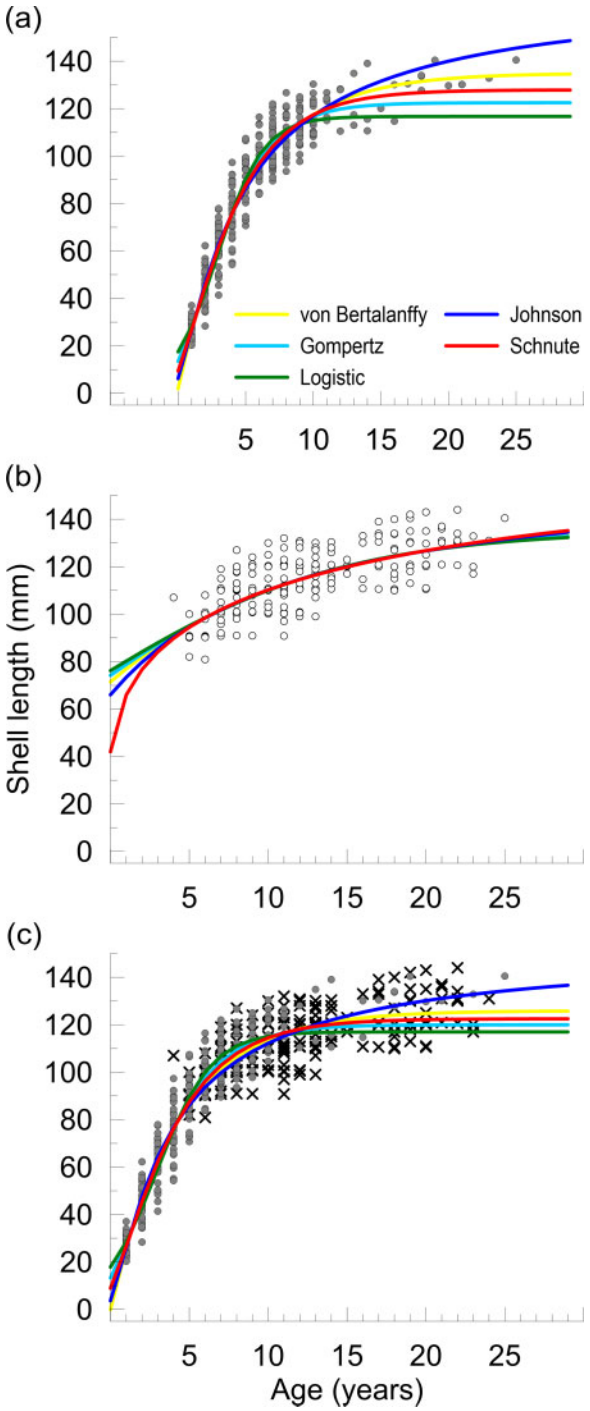

Figure 4. Candidate *Panopea generosa* growth models adjusted to the SL-to-age data obtained via different methods: (a) IGP (●; $n = 293$), (b) SLTA (○; $n = 243$), and (c) a combination of both IGP (●; $n = 293$) and SLTA (×; $n = 212$).

SLTA modelling

The fit of the five candidate growth models for the SLTA data set revealed similarly shaped curves, the trajectories of which followed the middle of the data projecting a similar L_∞ with values

Table 2. Parameters from the growth models fitted to three *Panopea generosa* SL-to-age data sets obtained via different methods and their respective bias corrected confidence intervals.

Model	Parameter	IGP	SLTA	IGP + SLTA
von Bertalanffy	L_∞ (mm)	135.0 (134.3 to 137.5)	139.1 (135.5 to 153.9)	125.9 (125.6 to 126.8)
	k	0.203 (0.189 to 0.212)	0.085 (0.052 to 0.105)	0.234 (0.223 to 0.241)
	t_0 (years)	−0.07 (−0.12 to 0.01)	−8.50 (−11.67 to −5.64)	0.00 (−0.05 to 0.07)
Gompertz	L_∞ (mm)	122.5 (122.5 to 123.6)	137.0 (133.9 to 148.6)	120.0 (119.8 to 120.3)
	k	0.384 (0.371 to 0.394)	0.103 (0.072 to 0.128)	0.394 (0.383 to 0.401)
	t_0 (years)	−0.43 (−0.60 to −0.28)	−26.76 (−40.38 to −19.24)	−0.36 (−0.56 to −0.23)
Logistic	L_∞ (mm)	116.7 (116.6 to 117.4)	135.3 (132.8 to 142.6)	117.0 (116.8 to 117.3)
	k	0.594 (0.566 to 0.615)	0.122 (0.096 to 0.147)	0.581 (0.559 to 0.598)
	t_0 (years)	2.93 (2.90 to 2.99)	−2.08 (−2.58 to −1.26)	2.95 (2.94 to 3.00)
Johnson	L_∞ (mm)	171.4 (169.5 to 175.2)	161.6 (155.3 to 184.8)	153.0 (152.0 to 155.2)
	k	0.232 (0.216 to 0.240)	0.150 (0.073 to 0.205)	0.296 (0.277 to 0.310)
	t_0 (years)	−1.30 (−1.46 to −1.14)	−7.46 (−14.15 to −4.09)	−0.90 (−1.00 to −0.77)
Schnute	L_∞ (mm)	127.9 (127.4 to 129.6)	155.7 (135.2 to 340.6)	122.5 (122.1 to 123.2)
	t_0 (years)	−1.00 (−2.13 to −0.25)	−0.20 (−16.35 to 2.07)	−0.97 (−2.16 to −0.24)
	β	0.537 (0.293 to 0.845)	3.909 (0.174 to 6.436)	0.516 (0.286 to 0.781)
	λ	0.282 (0.236 to 0.318)	0.029 (0.000 to 0.101)	0.307 (0.270 to 0.339)
	y_1 (mm)	26.7 (–)	89.8 (80.9 to 91.1)	26.6 (–)
	y_2 (mm)	127.7 (127.2 to 129.3)	131.9 (129.9 to 137.0)	122.4 (122.2 to 123.2)

Table 3. *AIC* and *SBC* rankings of five candidate growth models for three *Panopea generosa* SL-to-age data sets obtained from the same sample using different methods.

			AIC			***SBC***		
Method	**Model**	θ_i	**Value**	Δ_i	w_i **(%)**	**Value**	Δ_i	w_i **(%)**
IGP	Schnute	4	−831.4	0.0	94.4	−816.7	0.0	72.6
	von Bertalanffy	3	−824.5	6.9	3.0	−813.5	3.2	14.7
	Gompertz	3	−824.2	7.2	2.6	−813.2	3.5	12.5
	Johnson	3	−813.8	17.6	0.0	−802.7	13.9	0.1
	Logistic	3	−780.1	51.3	0.0	−769.1	47.6	0.0
SLTA	Johnson	3	−549.6	0.0	26.2	−539.2	0.0	28.5
	von Bertalanffy	3	−549.4	0.2	23.3	−538.9	0.2	25.3
	Gompertz	3	−549.2	0.4	21.4	−538.7	0.4	23.3
	Logistic	3	−549.0	0.6	19.4	−538.6	0.6	21.1
	Schnute	4	−547.6	2.0	9.7	−533.7	5.5	1.8
IGP + SLTA	Schnute	4	−819.2	0.0	90.2	−802.3	0.0	52.7
	Gompertz	3	−813.8	5.4	6.0	−801.1	1.2	28.9
	von Bertalanffy	3	−812.9	6.3	3.8	−800.2	2.1	18.4
	Johnson	3	−793.1	26.1	0.0	−780.4	21.9	0.0
	Logistic	3	−775.8	43.4	0.0	−763.1	39.2	0.0

θ_i, number of parameters that are used in each model.

ranging between 135.3 and 161.6 mm for the Logistic and Johnson growth models, respectively (Figure 4b and Table 2). The greatest differentiation in growth projections among candidate models occurs in the first years of development; precisely in those age classes for which data are lacking (1–3 years) or sparse (4–6 years). Thus, backward projections of the growth models for the first years of development resulted in intersection of the ordinate between 42 and 76 mm.

The *AIC* and *SBC* supported the Johnson model as the best model (Table 3). In addition, the Δ_i for the *AIC* and *SBC* indicated that the von Bertalanffy, Gompertz, and Logistic models were plausible predictors of individual growth ($\Delta_i \leq 0.6$). The *AIC* and *SBC* gave considerably less support to the Schnute model ($\Delta_i = 2.0$ and 5.5, respectively).

The *AIC* and *SBC* weights (w_i) indicated that four of the five analysed models yielded similar performance as alternative growth models (Table 3). The Schnute growth model was discarded as an alternative model ($w_{i\text{-}AIC} = 9.7\%$ and $w_{i\text{-}SBC} = 1.8\%$).

IGP + SLTA modelling

The growth trajectories described by the models fitted to the IGP + SLTA dataset described a similar pattern of growth in the first years of development of the individuals with a slight spread at the asymptotic phase (Figure 4c). The asymptotic phase was attained by the von Bertalanffy, Gompertz, and Schnute models at the age of 15 years. The logistic growth model reached this phase early at around 10 years, and the Johnson growth model reached asymptotic length at ages greater than those found in the population (>25 years).

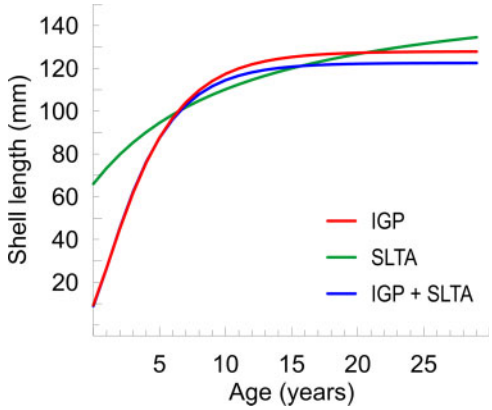

Figure 5. The most parsimonious model for each *Panopea generosa* data set: the Schnute growth model for the IGP data, the Johnson growth model for SLTA, and the Schnute growth model for IGP + SLTA.

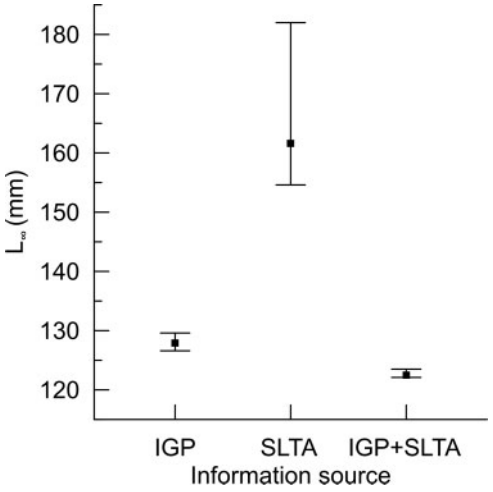

Figure 6. Asymptotic *Panopea generosa* SL values (L_∞) of each most parsimonious model and their respective upper and lower bias-corrected confidence intervals.

The *AIC* and *SBC* indicate that the Schnute growth model is the best descriptor of the data (Table 3). Moreover, for *AIC*, the Schnute model has a high percentage of evidence of support to describe the data ($w_{i\text{-}AIC}$ = 90.2%), with little support for the other models. In contrast, the *SBC* also supports the Gompertz and von Bertalanffy models as alternatives with substantial support ($w_{i\text{-}SBC}$ = 28.9% and 18.4%, respectively).

In summary, the three data sets and their respective most parsimonious models show clear differences in their growth curve trajectories, specifically during the early years of accelerated growth, and at the beginning of the asymptotic phase (Figure 5). The Johnson model performance was flawed in that the predicted asymptotic length (L_∞ = 161.9 mm) occurs during ages not found in the population (>25 years). In addition, SL predictions during the first years were vague, with the curve crossing the *y*-axis at 66 mm. Both criteria agreed in selecting the Schnute growth model as the winner for data sets that use IGP (IGP and IGP + SLTA data sets) with lower predicted asymptotic SLs (L_∞= 127.9 and 122.5 mm, respectively) reached at about 15 years. Both Schnute models crossed the *y*-axis with values close to zero (≈9 mm). Thus, the predictions of the Schnute growth model fitted to both IGP data sets revealed reasonable estimates of length at age during ontogenetic development according to the observed data. The asymptotic SLs (L_∞) estimated by the models show wide differences in their optimal value (up to 39 mm; Figure 6). The greatest value of L_∞ was generated from the SLTA dataset and is associated with the widest confidence interval. Meanwhile, the lowest values were found between closer confidence intervals, especially for the combined IGP + SLTA dataset.

Performance of the most parsimonious models

According to the r^2 values, the proportion of variance explained by the best fitted model is higher with the IGP and the IGP + SLTA data sets (>0.9; Table 4) than with SLTA data alone. In addition, the accuracy of the predicted data is higher with data sets IGP data according to the *ME* method (>0.9 in both case).

Analysis of temporal correlation of IGP data

The statistical relationship between ΔL_t and fitted values for the mixed-effects version of the Schnute growth model is shown in Figure 7. The Ljung–Box test was unable to falsify the null hypothesis of no temporal autocorrelation of residuals ($Q_{\alpha<0.5,\ df=1} = 0.187$ (p-value < 0.665). The Ψ_i matrix was estimated as:

$$\Psi_i = \begin{pmatrix} 2.03 & 0.002 & 0.0009 \\ 0.002 & 0.023 & 0.002 \\ 0.0009 & 0.002 & 0.0007 \end{pmatrix},$$

where the correlations for the parameters of the Schnute growth model including random effects were estimated as: (a) $\rho l_\infty \beta^\tau$ = 0.009, (b) $\rho l_\infty \lambda^\tau$ = 0.022, and (c) $\rho \beta \lambda^\tau$ = 0.046.

Table 4. Modelling performance of the three most parsimonious models fitted to the three *Panopea generosa* data sets.

			Test	
Data set	**Individuals**	**Selected model**	r^2	*ME*
IGP	31	Schnute	0.96	0.93
SLTA	243	Johnson	0.51	0.51
IGP + SLTA	274	Schnute	0.90	>0.99

Discussion

Improper management actions can result from low accuracy growth models. Accurate estimation of individual growth parameters in some long-lived species has been difficult, in part because sampling bias against small individuals leads to a paucity of size data from early age classes. Here, we evaluated growth modelling though the implementation and integration of IGP data with the current standard SLTA data for the Pacific geoduck, *Panopea generosa*. Our results reveal that the incorporation of IGP data in growth models yields significant improvement over models generated with SLTA data alone.

The probability of finding certain age groups in populations of long-lived bivalves, such as *Panopea* sp. and *Artica islandica*, is affected by some population traits, like prolonged longevity and high interannual variability in recruitment. In conjunction with

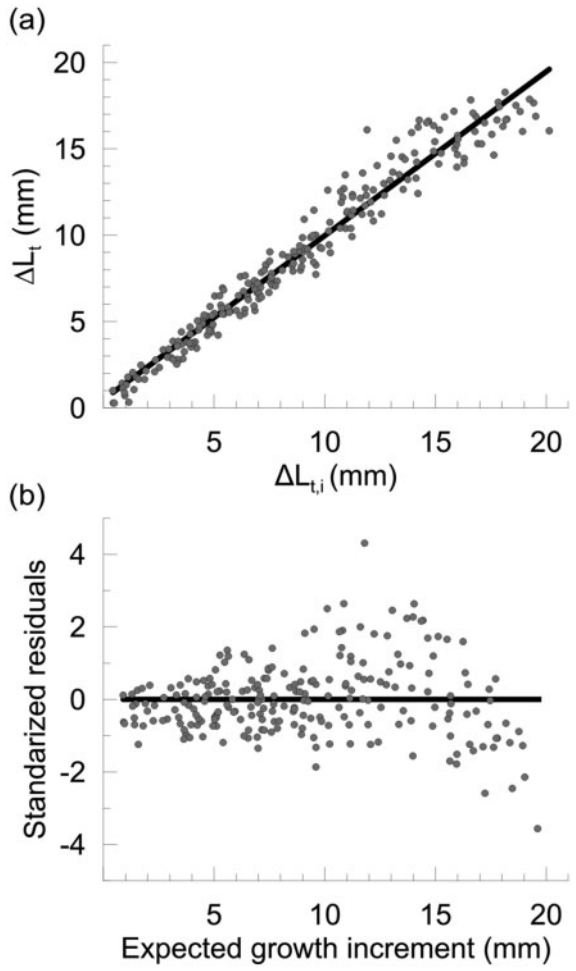

Figure 7. Scatter plots of (a) expected mean growth increment versus fitted values for the mixed-effects version of the Schnute growth model and (b) residuals of the Schnute growth model.

sampling bias, these factors result in a paucity of individuals belonging to the first age classes (Thórarinsdóttir and Einarsson, 1996; Orensanz *et al.*, 2004; Zhang and Campbell, 2004; Powell and Mann, 2005). For example, the age structures of *P. globosa* populations from Bahía Magdalena, BCS (González-Peláez *et al.*, 2015), and San Felipe, BC (Aragón-Noriega *et al.*, 2015), showed a dominance of older individuals (>12 and 19 years, respectively), suggesting that recruitment patterns were irregular. As a consequence, the representativeness of age classes was strongly biased toward the adult fraction of the population, limiting the capability to describe the accelerated phase of growth in the sample analysed. Given the limited information, the estimation of growth parameters could be biologically unrealistic and thus relatively uninformative. Interpretation of these approximate parameters can be problematic for the sustainable fisheries management, e.g. erroneous estimates of mortality and projections of biomass in the future (Hilborn and Walters, 1992; Chen, 2003; King, 2007).

To improve the estimates of the individual growth of the populations, combining additional sources of information with the data of the original sample (SLTA) have been explored. Seed and Brown (1978) and Adjei-Boateng and Wilson (2013) complemented the description of growth by integrating information from the analysis of the age frequency distribution with measurements of marked individuals and observed a degree of improvement in the performance of growth models. However, their results are subject to important limitations of the method: (i) the distribution of age frequencies is a subjective method that is inappropriate when individuals present high variability in growth rates that mask age differences (Richardson *et al.*, 1990) and (ii) the tag-recapture method is a time-consuming procedure that should generally be limited to areas excluded from fishing exploitation (Shaul and Goodwin, 1982). Luquin-Covarrubias *et al.* (2016) considered the incorporation of information from the first stages of development to the SLTA data. Although this procedure has the capacity to increase the accuracy of the estimates of the origin of the curve and give a better biological meaning to t_0, it is limited to the availability of information during the early ages (larvae, postlarvae, juveniles). In addition, the estimation of sizes of the individuals during the first years is only a projection of the origin of the curve.

In the present study, incorporation of length at age data in the first age classes clearly improved growth modelling performance (Table 4). We observed a direct effect on the estimated parameters, particularly the asymptotic length and the origin of the curve. Specifically, the L_∞ estimated from the fit of the Johnson model to the SLTA data alone is a greater SL than found in the population (161.9 mm), overestimating the average length at maximum age to a higher degree than the IGP and IGP + SLTA data sets. Both the IGP and IGP + SLTA analyses resulted in lower values of L_∞ estimated by the Schnute model (127.9 and 122.5 mm for IGP and IGP + SLTA, respectively), which are biologically reasonable as these lengths are attained at ages found in the population (around 15 years). Therefore, unlike the model based on SLTA alone, the inclusion of IGP data results in growth models with a more realistic estimation of L_∞. Estimates of the origin of the curve presented a better biological meaning as well (Figure 5): the curve origin of the Schnute model fitted to IGP and IGP + SLTA cross the ordinate closer to zero; as opposed to Johnson model fitted to the SLTA data, in which the ordinate is crossed at a much higher SL value (42–76 mm), which is biologically inappropriate as the length at birth is overestimated. The addition of IGP data yields a biologically relevant description of individual growth during the first years by giving growth curves a point of inflection. Thus, inferences of growth without representation of one or another side of the age structure can distort or bias the estimated growth parameters (Haddon, 2011; Smart *et al.*, 2013; D'Alberto *et al.*, 2017).

We observed that the inclusion of data with broader representation of age classes increased the discrimination capacity of the selection criteria. For example, since the fit of the models on the SLTA data alone was made in individuals who had already reached their adult sizes (or were very close to reaching it), the trajectories of the candidate models were very similar to each other. Therefore, although Johnson was the most parsimonious model using SLTA data alone according to both selection criteria, the remaining candidate models were equally viable as alternative functions. On the other hand, among models that involved the implementation of the IGP (IGP and IGP + SLTA), Schnute was the most parsimonious model according to both criteria. The SBC also considered an alternative model (Gompertz) primarily because the SBC tends to select more parsimonious models (Burnham, 2004). As both selection criteria were in accord, it gives assurance on the robustness of the choice and no further

search for additional models is required (Kuha, 2004). Furthermore, growth models fitted to the more informative data sets have stronger relationships ($r^2 > 0.9$) and are more accurate ($ME > 0.9$) to describe the individual growth than those fitted only to terminal data ($r^2 = 0.51$; $ME = 0.51$).

Our results illustrate the importance of including data that cover all age ranges; Hilborn and Walters (1992) pointed out that length-at-age data are more informative for the modelling of growth with adequate representation of the population's growth structure. In a previous study in Punta Canoas, the age structure of the sample obtained from the commercial fishery comprised age groups from 4 to 25 years (Hidalgo-de-la-Toba *et al.*, 2015). A directed sampling focused on the bycatch of the commercial fishery was carried out to increase the representation of young individuals in the sample. By incorporating ages ranging from 2 to 6 years, it was possible to get a plausible estimate of the predicted length in the early years and determine the asymptotic length (137 mm). Here, by working with the same samples from the commercial fishery, it was possible to increase the information of SL-at-age between the ages of 1 and 10 years, improving the accuracy of the asymptotic length (122–127 mm). To achieve this, additional samples were unnecessary.

The evidence presented herein suggests the need to reanalyse previous estimates of growth in populations that lack adequate age representation. A clear advantage of the IGP method (in addition to incorporating SL data for younger age classes) is that it obviates the need for additional samples since it can be done with specimens already collected. Indeed, shells used in previous growth studies and stored in collections can be analysed again with IGP and their results can be compared. The IGP method is well suited to long-lived clams that only exhibit interannual growth and lack seasonal migrations that could modify its population structure (Shaul and Goodwin, 1982). Furthermore, because this fishery is non-selective above a certain size threshold, individuals from almost all older age classes contain the valuable IGP information for the smaller age classes.

There are a few limitations of this method. The first is erosion and damage to the shell due to burrow abrasion and/or sample preparation. Although annuli could still be visible in cross-sections, the exact point where they ended could be hard to determine if there are discontinuities. Also, if external annuli are eroded their subsequent measure could be misleading. We recommend discarding samples that generate doubts in the readings. In addition, since IGP are multiple SL measurements on each subject (i.e. longitudinal data), these data can be auto-correlated due to intrinsic differences among individuals and environmental factors, which are persistent and/or recurrent trough time (Escati-Peñaloza *et al.*, 2010). Thus, serial correlation must be accounted for to generate a proper analysis. In this study, we found no evidence indicating that growth measurements in the same individual (longitudinal data) were auto-correlated. This information is relevant to modelling growth in *Panopea* spp. because IGP data have the advantage that they provide valuable information on growth variability (between-individual and within-individual), especially during the early years of accelerated growth. Thus, the IGP longitudinal data adequately compensate for the absence of ages and sizes for younger individuals of *P. generosa*, as a consequence of sampling obtained from fishery-dependent data, which did not harvest young clams.

The procedure based on the IGP method differs from back-calculations of size-at-age as used in fishes. According to Francis (1990), back-calculation is a technique that uses a set of measurements made on a hard part of a fish at one time, to infer its length at an earlier time or times. The requirements of back-calculations of size-at-age include an estimation procedure based on different equations (e.g. linear, exponential, quadratic, or non-linear). The data obtained for IGP are not obtained from mathematical equations but are empirically measured for each geoduck. The IGP procedure potentially helps to distinguish both internal and external growth marks in each individual to recover length-at-age data; as proposed by Escati-Peñaloza *et al.* (2010) for the striped clam *Ameghimonya antiqua*. Millstein and O'Clair (2001) remarked that longitudinal data are also more powerful for studying temporal and year-class effects on growth than age-length data, because the growth estimates are based on a more restricted period of time.

Summary

In a management context, our results show that the incorporation of IGP data yields reliable information about individual growth from a smaller number of organisms: although only 31 individuals were used for IGP, the number of SL-to-age data is still higher (293) than that in SLTA where 243 clams were used. Thus, precise descriptions of individual growth can be obtained with a lower budget and in less time than with SLTA (less processing time and smaller sample sizes). For some species, these attributes would be useful when access to populations is restricted by their low number, high value, difficult geographical or bathymetric access, or reduced impacts (e.g. fossil shells from museum collections).

Acknowledgements

The authors thank Eduardo Balart-Páez and Noemí Bocanegra-Castillo for support in the CIBNOR and José García and Raúl García for their help with fieldwork. The authors thank two anonymous reviewers for their constructive comments that improved the content and presentation of our study.

Funding

The authors gratefully acknowledge Consejo Nacional de Ciencia y Tecnología for support received throughout the projects (contract A1-S-36410) and a fellowship to J.A.H.-d.-l.-T. (grant no. 279953).

Data availability statement

The data underlying this article will be shared on reasonable request to the corresponding author.

References

Adjei-Boateng, D., and Wilson, G. J. 2013. Age determination and growth rate of the freshwater clam *Galatea paradoxa* (Born 1778) from the Volta River estuary, Ghana. Journal of Aquatic Science, 1: 31–38.

Aragón-Noriega, E. A., Calderon-Aguilera, L. E., and Pérez-Valencia, S. A. 2015. Modeling growth of the Cortes geoduck *Panopea globosa* from unexploited and exploited beds in the northern Gulf of California. Journal of Shellfish Research, 34: 119–127.

Barreto, R. R., Lessa, R. P., Hazin, F. H., and Santana, F. M. 2011. Age and growth of the blacknose shark, *Carcharhinus acronotus* (Poey, 1860) off the northeastern Brazilian Coast. Fisheries Research, 110: 170–176.

Bautista-Romero, J. J., González-Peláez, S. S., Morales-Bojórquez, E., Hidalgo-De-La-Toba, J. A., and Lluch-Cota, D. B. 2015. Sinusoidal Function Modeling Applied to Age Validation of

Geoducks Panopea generosa and Panopea globosa. Journal of Shellfish Research, 34: 21–29.

Breen, P. A., Gabriel, C., and Tyson, T. 1991. Preliminary estimates of age, mortality, growth, and reproduction in the hiatellid clam *Panopea zelandica* in New Zealand. New Zealand Journal of Marine and Freshwater Research, 25: 231–237.

Bureau, D., Hajas, W., Scurry, N. W., Hand, C. M., Dovey, G., and Campbell, A. 2002. Age, size structure and growth parameters of geoducks (*Panopea abrupta*, Conrad 1849) from 34 Locations in British Columbia sampled between 1993 and 2000. Canadian Technical Report of Fisheries and Aquatic Sciences, 2413: 84.

Bureau, D., Hajas, W., Hand, C. M., and Dovey, G. 2003. Age, size structure and growth parameters of geoducks (*Panopea abrupta*, Conrad 1849) from seven locations in British Columbia sampled in 2001 and 2002. Canadian Technical Report of Fisheries and Aquatic Sciences, 2494: 29.

Burnham, K. P. 2004. Multimodel Inference: Understanding AIC and BIC in Model Selection. Sociological Methods & Research, 33: 261–304.

Burnham, K. P., and Anderson, D. R. 2002. Model Selection and Multimodel Inference: A Practical Information-Theoretic Approach. Springer-Verlag, New York. 488 pp.

Calderon-Aguilera, L. E., Aragón-Noriega, E. A., Hand, C. M., and Moreno-Rivera, V. M. 2010. Morphometric relationships, age, growth, and mortality of the geoduck clam, *Panopea generosa*, along the Pacific coast of Baja California, Mexico. Journal of Shellfish Research, 29: 319–326.

Calderon-Aguilera, L. E., Aragón-Noriega, E. A., Morales-Bojórquez, E., Alcántara-Razo, E., and Chávez-Villalba, J. 2014. Reproductive cycle of the geoduck clam *Panopea generosa* at its southernmost distribution limit. Marine Biology Research, 10: 61–72.

Campana, S. E. 1990. How reliable are growth back-calculations based on otoliths? Canadian Journal of Fisheries and Aquatic Sciences, 47: 2219–2227.

Campbell, A., and Ming, M. D. 2003. Maturity and growth of the Pacific geoduck clam, *Panopea abrupta*, in southern British Columbia, Canada. Journal of Shellfish Research, 22: 85–90.

Cerrato, R. M. 2000. What fish biologists should know about bivalve shells. Fisheries Research, 46: 39–49.

Chang, W. Y. B. 1982. A statistical method for evaluating the reproducibility of age determinación. Canadian Journal of Fisheries and Aquatic Sciences, 39: 1208–1210.

Chen, Y. 2003. Quality of fisheries data and uncertainty in stock assessment. Scientia Marina, 67: 75–87.

D'Alberto, B. M., Chin, A., Smart, J. J., Baje, L., White, W. T., and Simpfendorfer, C. A. 2017. Age, growth and maturity of oceanic whitetip shark (*Carcharhinus longimanus*) from Papua New Guinea. Marine and Freshwater Research, 68: 1118–1129.

Deriso, R. B., Quinn, T. J. II, and Neal, P. R. 1985. Catch-age analysis with auxiliary information. Canadian Journal of Fisheries and Aquatic Sciences, 42: 815–824.

Escati-Peñaloza, G., Parma, A. M., and Orensanz, J. M. L. 2010. Analysis of longitudinal growth increment data using mixed-effects models: Individual and spatial variability in a clam. Fisheries Research, 105: 91–101.

Fournier, D., and Archibald, C. P. 1982. A general theory for analyzing catch at age data. Canadian Journal of Fisheries and Aquatic Sciences, 39: 1195–1203.

Francis, R. I. C. C. 1990. Back-calculation of fish length: a critical review. Journal of Fish Biology, 36: 883–902.

Gerasimova, A. V., and Maximovich, N. V. 2013. Age-size structure of common bivalve mollusc populations in the White Sea: the causes of instability. Hydrobiologia, 706: 119–137.

Gimenez, L. H., Doldan, M. d. S., Zaidman, P. C., and Morsan, E. M. 2020. Age and growth of *Glycymeris longior* (Sowerby, 1832) clam at the southern edge of its distribution (Argentine Sea). Helgoland Marine Research, 74:2.

González-Peláez, S. S., Leyva-Valencia, I., Pérez-Valencia, S., and Lluch-Cota, D. B. 2013. Distribution limits of the geoduck clams *Panopea generosa* and *P. globosa* on the Pacific coast of Mexico. Malacologia, 56: 85–94.

González-Peláez, S. S., Morales-Bojórquez, E., Lluch-Cota, D. B., Lluch-Cota, S. E., and Bautista-Romero, J. J. 2015. Modeling geoduck growth: multimodel inference in *Panopea globosa* from the southwestern Baja California Peninsula, Mexico. Journal of Shellfish Research, 34: 101–112.

Haddon, M. 2011. Modelling and Quantitative Methods in Fisheries. CRC Press, Boca Raton, Florida. 433 pp.

Haist, V. 2018. Analysis of paua (*Haliotis iris*) maturity and growth. New Zealand Fisheries Assessment Report 2018/21. 44 pp.

Hidalgo-de-la-Toba, J. A., González-Peláez, S. S., Morales-Bojórquez, E., Bautista-Romero, J. J., and Lluch-Cota, D. B. 2015. Geoduck *Panopea generosa* growth at its southern distribution limit in North America using a multimodel inference approach. Journal of Shellfish Research, 34: 91–99.

Hidalgo-de-la-Toba, J. A., Morales-Bojórquez, E., González-Peláez, S. S., Bautista-Romero, J. J., and Lluch-Cota, D. B. 2018. Modeling the temporal periodicity of growth increments based on harmonic functions. PLoS One, 13: e0196189.

Hilborn, R., and Walters, C. J. 1992. Quantitative Fisheries Stock Assessment: Choice, Dynamics and Uncertainty. Chapman & Hall, Inc., New York. 570 pp.

Hoffman, A., Bradbury, A., and Goodwin, C. L. 2000. Modeling geoduck, *Panopea abrupta* (Conrad, 1849) population dynamics. I. Growth. Journal of Shellfish Research, 19: 57–62.

Jacobson, L. D., Lo, N. C. H., and Barnes, J. T. 1994. A biomass-based assessment model for northern anchovy, *Engraulis mordax*. Fishery Bulletin, 92: 711–724.

Johnson, J. B., and Omland, K. S. 2004. Model selection in ecology and evolution. Trends in Ecology & Evolution, 19: 101–108.

Jones, D. S., Thompson, I., and Ambrose, W. 1978. Age and growth rate determinations for the Atlantic surf clam *Spisula solidissima* (Bivalvia: Mactracea), based on internal growth lines in shell cross-sections. Marine Biology, 47: 63–70.

Katsanevakis, S. 2006. Modelling fish growth: model selection, multi-model inference and model selection uncertainty. Fisheries Research, 81: 229–235.

Kilada, R. 2010. Validated age and growth estimates of two clam species in a saltwater lake on the Suez Canal in Egypt. Egyptian Journal of Aquatic Biology and Fisheries, 14: 111–126.

Kilada, R. W., Roddick, D., and Mombourquette, K. 2007a. Age determination, validation, growth and minimum size of sexual maturity of the Greenland smoothcockle (*Serripes groenlandicus*, Bruguiere, 1789) in Eastern Canada. Journal of Shellfish Research, 26: 443–450.

Kilada, R. W., Campana, S. E., and Roddick, D. 2007b. Validated age, growth, and mortality estimates of the ocean quahog (*Arctica islandica*) in the western Atlantic. ICES Journal of Marine Science, 64: 31–38.

King, M. 2007. Fisheries Biology, Assessment and Management. Blackwell Publishing, Oxford, UK. 382 pp.

Kuha, J. 2004. AIC and BIC: Comparisons of Assumptions and Performance. Sociological Methods & Research, 33: 188–229.

Lessa, R., and Duarte-Neto, P. 2004. Age and growth of yellowfin tuna (*Thunnus albacares*) in the western equatorial Atlantic, using dorsal fin spines. Fisheries Research, 69: 157–170.

Leyva-Valencia, I., Cruz-Hernández, P., Álvarez-Castañeda, S. T., Rojas-Posadas, D. I., Correa-Ramírez, M. M., Vadopalas, B., and Lluch-Cota, D. B. 2015. Phylogeny and Phylogeography of the Geoduck *Panopea* (Bivalvia: Hiatellidae). Journal of Shellfish Research, 34: 11–20.

Lindstrom, M. J., and Bates, D. M. 1990. Nonlinear Mixed Effects Models for Repeated Measures Data. Biometrics, 46: 673–687.

Link, W. a., and Barker, R. J. 2006. Model weights and the foundations of multimodel inference. Ecology, 87: 2626–2635.

Ljung, G. M., and Box, G. E. P. 1978. On a measure of lack of fit in time series models. Biometrika, 65: 297–303.

Loague, K., and Green, R. E. 1991. Statistical and graphical methods for evaluating solute transport models: overview and application. Journal of Contaminant Hydrology, 7: 51–73.

Luquin-Covarrubias, M. A., Morales-Bojórquez, E., González-Peláez, S. S., and Lluch-Cota, D. B. 2016. Joint likelihood function based on multinomial and normal distributions for analyzing the phenotypic growth variability of geoduck clam *Panopea globosa*. California Cooperative Oceanic Fisheries Investigations Reports, 57: 151–162.

Millstein, J., and O'Clair, C. E. 2001. Comparison of age-length and growth-increment general growth models of the Schnute type in the Pacific Blue Mussel, *Mytilus trossulus* Gould. Journal of Experimental Marine Biology and Ecology, 262: 155–176.

Neter, J., Kutner, M. H., Nachtschien, J., and Wasserman, W. 1996. Applied Linear Statistical Models. McGraw-Hill/Irwin, Chicago. 1408 pp.

Orensanz, J. M. L., Hand, C. M., Parma, A. M., and Valero, J. 2004. Precaution in the harvest of Methuselah's clams—the difficulty of getting timely feedback from slow-paced dynamics. Canadian Journal of Fisheries and Aquatic Sciences, 61: 1355–1372.

Pardo, S. A., Cooper, A. B., and Dulvy, N. K. 2013. Avoiding fishy growth curves. Methods in Ecology and Evolution, 4: 353–360.

Powell, E. N., and Mann, R. 2005. Evidence of recent recruitment in the ocean quahog *Arctica islandica* in the Mid-Atlantic Bight. Journal of Shellfish Research, 24: 517–530.

R Core Team. 2020. R: A Language and Environment for Statistical Computing. R Foundation for Statistical Computing, Vienna, Austria.

Richardson, C. A., Seed, R., and Naylor, E. 1990. Use of internal growth bands for measuring individual and population growth rates in *Mytilus edulis* from offshore production platforms. Marine Ecology Progress Series, 66: 259–265.

Ricker, W. E. 1979. Growth rates and models. In Fish Physiology, VIII, pp. 677–743. Ed. by W. S. Hoar, D. J. Randall, and J. R. Brett. Academic Press, Inc., New York.

Ricker, W. E. 1992. Back-calculation of fish lengths based on proportionality between scale and length increments. Canadian Journal of Fisheries and Aquatic Sciences, 49: 1018–1026.

Schöne, B. R., Dunca, E., Fiebig, J., and Pfeiffer, M. 2005. Mutvei's solution: an ideal agent for resolving microgrowth structures of biogenic carbonates. Palaeogeography, Palaeoclimatology, Palaeoecology, 228: 149–166.

Seed, R., and Brown, R. A. 1978. Growth as a strategy for survival in two marine bivalves, *Cerastoderma edule* and *Modiolus modiolus*. Journal of Animal Ecology, 47: 283–292.

Shaul, W., and Goodwin, L. 1982. Geoduck (*Panope generosa*: Bivalvia) age as determined by internal growth lines in the shell. Canadian Journal of Fisheries and Aquatic Sciences, 39: 632–636.

Smart, J. J., Harry, A. V., Tobin, A. J., and Simpfendorfer, C. A. 2013. Overcoming the constraints of low sample sizes to produce age and growth data for rare or threatened sharks. Aquatic Conservation: Marine and Freshwater Ecosystems, 23: 124–134.

Smith, J., Smith, P., and Addiscott, T. 1996. Quantitative methods to evaluate and compare Soil Organic Matter (SOM) models. *In* Evaluation of Soil Organic Matter Models Using Existing Long-Term Datasets, Harpenden, Hertfordshire, UK. Ed. by D. S. Powlson, P. Smith and J. U. Smith. Springer-Verlag Berlin Heidelberg, pp. 181–199.

Thompson, I., Jones, D. S., and Dreibelbis, D. 1980. Annual internal growth banding and life history of the ocean quahog *Arctica islandica* (Mollusca: Bivalvia). Marine Biology, 57: 25–34.

Thórarinsdóttir, G. G., and Einarsson, S. T. 1996. Distribution, abundance, population structure and meat yield of the ocean quahog, *Arctica islandica*, in icelandic waters. Journal of the Marine Biological Association of the United Kingdom, 76: 1107–1114.

Thorson, J. T., and Simpfendorfer, C. A. 2009. Gear selectivity and sample size effects on growth curve selection in shark age and growth studies. Fisheries Research, 98: 75–84.

Wang, Y., and Liu, Q. 2006. Comparison of Akaike information criterion (AIC) and Bayesian information criterion (BIC) in selection of stock–recruitment relationships. Fisheries Research, 77: 220–225.

Ward, E. J. 2008. A review and comparison of four commonly used Bayesian and maximum likelihood model selection tools. Ecological Modelling, 211: 1–10.

Weymouth, F. W. 1923. The life-history and growth of the Pismo clam (*Tivela stultorum* Mawe). California Fish and Game Commission, Fish Bulletin No, 7: 1–119.

Weymouth, F. W., and McMillin, H. C. 1930. The relative growth and mortality of the Pacific azor clam (*Siliqua patula*, Dixon), and their bearing on the commercial fishery. Bulletin of the Bureau of Fisheries, 1099: 567.

Zaidman, P. C., and Morsan, E. 2015. Growth variability in a metapopulation: the case of the southern geoduck (*Panopea abbreviata*). Fisheries Research, 172: 423–431.

Zhang, Z., and Campbell, A. 2004. Natural mortality and recruitment rates of the Pacific geoduck clam (*Panopea abrupta*) in experimental plots. Journal of Shellfish Research, 23: 675–682.

Zhang, Z., and Hand, C. 2006. Recruitment patterns and precautionary exploitation rates for geoduck (*Panopea abrupta*) populations in British Columbia. Journal of Shellfish Research, 25: 445–453.

Handling editor: Emory Anderson